Electrical Postcompensation of SOA Impairments for Fiber-Optic Transmission

Xiaoxu Li and Guifang Li, *Senior Member, IEEE*

***Abstract*—An electrical postcompensation scheme for semiconductor optical amplifier (SOA) impairments has been proposed. An on–off keying transmission over 100-km standard single-mode fiber and three SOAs was demonstrated experimentally with SOA impairment compensation. An 8-dB improvement in Q-factor has been achieved.**

***Index Terms*—Data pattern effect, on–off keying (OOK), self-phase modulation (SPM), semiconductor optical amplifiers (SOAs).**

I. Introduction

THE semiconductor optical amplifier (SOA) has attracted much attention as a potential substitute for the erbium-doped fiber amplifier for optical transmission due to its low cost, compactness, and ultrawide gain spectrum. It is also the only mature technology for providing amplification in the 1310-nm transmission window. A few transmission experiments using SOAs have been demonstrated using both on–off keying (OOK) and differential phase-shift keying in the 1310- and 1550-nm windows [1]–[4]. The performance in such systems was mainly limited by the amplified spontaneous emission (ASE) noise and nonlinear impairments of the SOA. When the signal power or launching power is low, the systems suffer from the rapid degradation of the signal-to-noise ratio (SNR) at the receiver due to accumulated ASE noise of SOAs along the link. When the signal power is high, SOAs will be saturated and the signals will suffer from the data pattern effect or self-gain modulation, self-phase modulation (SPM), and interchannel crosstalk effects such as cross-gain modulation (XGM) and four-wave mixing (FWM) through SOAs in wavelength-division multiplexing (WDM). In order to maximize the SNR of the received signals while maintaining system performance, SOA nonlinearities need to be compensated. Currently electrical postcompensation of fiber impairments has become available aided by coherent detection and digital signal processing (DSP) technique [5], [6]. In this letter, we propose, for the first time to our knowledge, an electrical postcompensation scheme for SOA impairments and demonstrate experimentally SOA impairment compensation (IC) in a nonreturn-to-zero (NRZ) transmission system.

Manuscript received December 15, 2008; revised January 29, 2009. First published February 24, 2009; current version published April 15, 2009. This work was supported in part by Defense Advanced Research Projects Agency (DARPA) under Contract DAAD1702C0097.

The authors are with CREOL, The College of Optics and Photonics, University of Central Florida, Orlando, FL 32816 USA (e-mail: xiali@creol.ucf.edu; li@creol.ucf.edu).

Color versions of one or more of the figures in this letter are available online at http://ieeexplore.ieee.org.

Digital Object Identifier 10.1109/LPT.2009.2015149

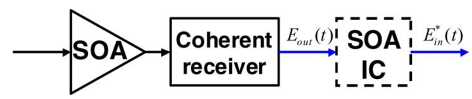

Fig. 1. Diagram of a single SOA IC. Optical path: black line. Electrical path: blue line.

II. Principle of SOA IC

Fig. 1 shows the schematic diagram of a single SOA IC. The intensity $P(z,\tau)$, phase $\phi(z,\tau)$, and gain $g(z,\tau)$ of the signal along the SOA can be described by [7]

$$\frac{\partial P}{\partial z} = (g - \alpha_{\rm int})P \tag{1}$$

$$\frac{\partial \phi}{\partial z} = -\frac{1}{2}\alpha_H g \tag{2}$$

$$\frac{\partial g}{\partial t} = \frac{g_0 - g}{\tau_c} - \frac{gP}{E_{\rm sat}} \tag{3}$$

where $\alpha_{\rm int}, \alpha_H, g_0, \tau_c, E_{\rm sat}$ are the internal loss, linewidth enhancement factor, small-signal gain coefficient, spontaneous carrier lifetime, and saturation energy of the SOA, respectively. $E_{\rm out}(t)$ is the measured output electrical field of the SOA after coherent detection. The proposed IC scheme is based on propagating the distorted signal backward in a virtual SOA in the digital domain by replacing $\partial/\partial z$ with $\partial/\partial(-z)$ in (1)–(3), which is equivalent to reverse the signs of gain and loss as follows:

$$\frac{\partial P}{\partial z} = (g^{'} - \alpha_{\rm int}^{'})P \tag{4}$$

$$\frac{\partial \phi}{\partial z} = -\frac{1}{2}\alpha_H g^{'} \tag{5}$$

$$\frac{\partial g^{'}}{\partial t} = \frac{g_0^{'} - g^{'}}{\tau_c} - \frac{g^{'}P}{E_{\rm sat}} \tag{6}$$

where $g^{'} = -g, \alpha_{\rm int}^{'} = -\alpha_{\rm int}, g_0^{'} = -g_0$. Integrating (6) over the SOA length (L) and making use of (4) to eliminate the product $g^{'}P$ by ignoring $\alpha_{\rm int}^{'}$ and the spatial dependence of the carrier lifetime τ_c along the SOA, the overall dynamics for $g^{'}$ in the SOA IC can be obtained as follows:

$$\left(1 + \tau_c \frac{d}{dt}\right) h^{'}(t) = h_0^{'} - \frac{P_{\rm out}(t)}{P_{\rm sat}}(\exp[h^{'}(t)] - 1) \tag{7}$$

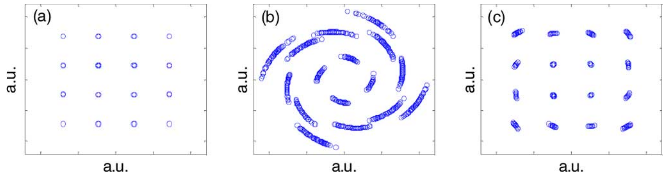

Fig. 2. Constellation of 16QAM signal (a) before SOA; (b) after SOA without IC; (c) after SOA with IC.

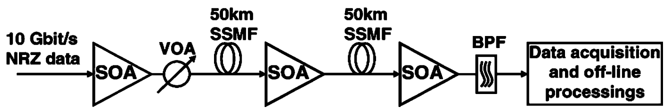

Fig. 3. Experimental setup of 1310-nm transmission with SOA IC. VOA: variable optical attenuator. BPF: bandpass filter.

where $h^{'}(t) = \int_0^L g^{'}(z,t)dz$ and $h_0^{'} = -g_0 L = -\ln G_0$; G_0 is the small-signal gain of the SOA. $P_{\rm sat} = E_{\rm sat}/\tau_c$ is the saturation output power of the SOA. $P_{\rm out}(t) = |E_{\rm out}(t)|^2$ is the output signal intensity of the physical SOA and the input for the SOA IC. Solving (4), (5), and (7), the electric field of the signal after IC can be written as

$$E_{\rm in}^{*}(t) = E_{\rm out}(t) \cdot \exp\left[\frac{(1-i\alpha_H)h^{'}(t)}{2}\right]. \qquad (8)$$

To demonstrate the feasibility of the SOA IC scheme, an optical 10-Gsym/s 16 quadrature amplitude modulation (QAM) signal transmission through a saturated SOA with SOA IC was simulated. The 16QAM transmitter and SOA were simulated using the VPI TransmissionMaker. The SOA module was based on the transmission line model with a small-signal gain of 21.8 dB and a saturation output power of 9.8 dBm at the injection current of 120 mA. ASE noise of the SOA was ignored for simplification. SOA IC was implemented by solving (7) numerically using the fourth-order Runge–Kutta method. Fig. 2(a) and (b) shows the constellations of the 16QAM signal before and after the saturated SOA. The corresponding average signal powers are -9 and 9.8 dBm, respectively. The constellation in Fig. 2(b) rotates due to the SPM effect through the SOA and the radial and angular spreads in each cluster of the constellation arise from the data pattern effect due to gain saturation of the SOA. Fig. 2(c) indicates that both the SPM effect and the data pattern effect are compensated effectively with SOA IC.

The proposed SOA IC scheme here can be universal for any modulation format with coherent detection. However, coherent detection might not be required in an intensity-modulation system where the SOA nonlinearities are dominant and the signal is not distorted from fiber, which is the case in the following transmission experiment.

III. Experimental Setup and Results

Fig. 3 shows the experimental setup for a 1310-nm NRZ transmission experiment over 100-km standard single-mode fiber (SSMF) with electrical postcompensation for SOA impairments. A 10-Gb/s NRZ signal was generated by externally modulating a 1310-nm distributed-feedback (DFB) laser with $2^{15}-1$ pseudorandom binary sequence (PRBS) data from a pulse pattern generator. The first bulk SOA having a small-signal gain of 23.5 dB and a saturation output power of 12 dBm at the injection current of 180 mA worked as a power booster. The variable optical attenuator was used to control the launching power into fiber. The transmission link was composed of two spans of 50-km SSMFs, each of which was followed by a bulk SOA to compensate the fiber loss. The measured fiber losses at 1310 nm were 17.4 and 18.4 dB, respectively. At an injection current of 120 mA, these two SOAs had small-signal gains of 24 and 23.5 dB and saturation output powers of 10 and 7 dBm, respectively. An optical bandpass filter with a 3-dB bandwidth of 7 nm was used to remove the ASE noise before photodetection. At each launching power, the signal power evolution throughout the transmission link were monitored by an optical powermeter to obtain the SOAs gain and the intensities of the received NRZ signals were acquired by an Agilent high-speed sampling oscilloscope after photodetection. The SOA IC was implemented off-line in the software domain. Direct detection, instead of coherent detection, was used before SOA IC here because the intensity-modulated signal are not distorted from fiber due to negligible chromatic dispersion of SSMF at 1310 nm thus signal phase is not necessary for SOA IC.

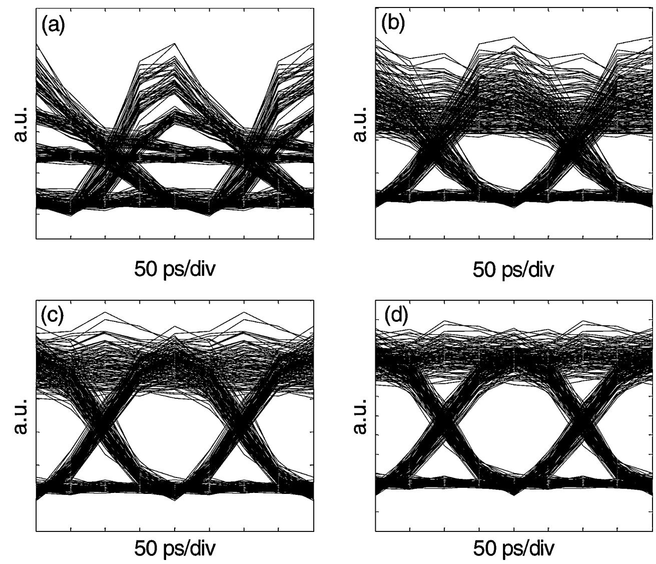

Fig. 4. Eye diagrams of (a) the received NRZ signal and the signal after IC for (b) one SOA; (c) two SOAs; (d) three SOAs.

Due to spectral broadening mainly through the SOAs from SPM, the received NRZ data were measured and sampled by the sampling oscilloscope at 27 GSa/s. In off-line processings for SOA IC, the data were first up-sampled to 40 GSa/s or 4 Sa/bit for higher temporal resolution. An ideal noiseless amplifier was assumed between two adjacent SOAs to compensate fiber loss. For IC for each SOA, (7) was solved numerically using the fourth-order Runge–Kutta method with measured small-signal gain and saturation output power of the SOA. At each launching power, the carrier lifetimes of the three SOAs were optimized through global search by maximizing the eye opening after IC.

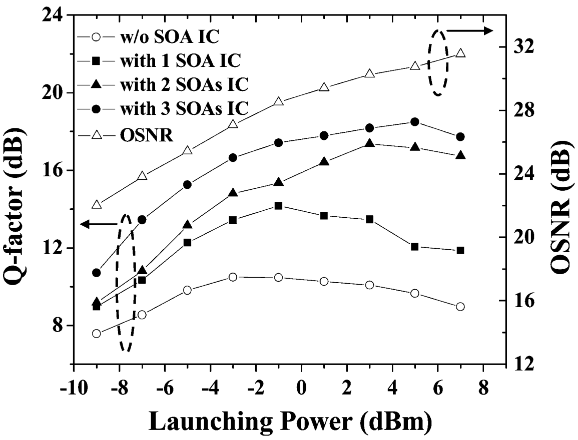

Fig. 5. Q-factor and OSNR versus launching power.

After IC for each SOA, the eye-diagram of the compensated signal was plotted. Fig. 4(a) shows the eye diagram of the received NRZ signal after transmission over 100-km SSMF when the launching power into fiber is 5 dBm. Strong pattern effect can be observed due to the accumulated SOA impairments; the eye is almost closed. Some of the pattern effect is compensated after IC for the preamplifying SOA, shown in Fig. 4(b). The SOA impairments are further compensated after IC for the in-line SOA, shown in Fig. 4(c). After IC for the power boostering SOA, shown in Fig. 4(d), only negligible pattern effect remains in the signal. The optimized carrier lifetimes in IC for the three SOAs are 150, 321, and 339 ps, respectively.

The dependence of the measured optical signal-to-noise ratio (OSNR) of the received signal in the optical bandwidth of 0.1 nm and the calculated Q-factor on the optical launching power is shown in Fig. 5. The received NRZ signals suffer from the accumulated ASE noise at low launching powers and SOAs nonlinearities at high launching powers, respectively. The optimum launching power is about -2 dBm with the Q-factor of 10.5 dB without IC. The optimum launching power and the corresponding Q-factor are both increased after each SOA IC. After IC for all three SOAs, the optimum launching power is increased to 5 dBm with the Q-factor of 18.5 dB. Compared to the Q-factor of the signal at back-to-back (22.9 dB), the 4.4-dB difference is mainly due to the presence of the accumulated ASE noise in the received signals, which cannot be compensated. The performance can be further improved by using optical filters after each SOA to remove the excess ASE noise.

IV. Conclusion and Discussion

In conclusion, an electrical postcompensation scheme for SOA impairments has been proposed. Transmission of OOK signal incorporating SOA IC has been demonstrated experimentally. The optimum launching power was increased by 7 dB and the Q-factor of the received NRZ signal was improved by 8 dB with SOA IC. The proposed SOA IC scheme is universal for any modulation format. The fourth-order Runge–Kutta algorithm is realized by multiplications, summations, and exponential calculations thus SOA IC can be implemented in digital domain using DSP in application-specific integrated circuit chips with multiply accumulate units and lookup tables. The digital processing speed of 40 GHz was used in the experiment to make the SOA IC effective; however, the DSP speed may be reduced by parallel processings. Coherent detection might not be necessary under some circumstances such as in the current experiment. However, when fiber dispersion is present, signals will be distorted through the interactions of fiber nonlinearities and dispersion; therefore, signal phase is required through coherent detection to compensate the impairments in fiber and SOA simultaneously. Furthermore, in WDM systems, the full rate equation model for SOAs and the coupled wave equations need to be used. The full knowledge of the exact bit sequences of the WDM channels is required to compensate interchannel effects such as XGM and FWM through SOAs effectively.

Recently maximum likelihood sequence estimation has been employed to increase tolerance to SOA nonlinearities [8]. This method requires a Viterbi decoding procedure whose computation requirement increases exponentially with the accumulated SOA impairments and becomes unacceptable for high spectral efficiency modulation formats such as QAM. For example, the calculations required for decoding one symbol of a 16QAM signal using a Viterbi decoder with a channel memory of three symbols involve 61 440 comparisons, 4096 summations, and 65 536 look-ups. Moreover, it cannot mitigate interchannel nonlinearities through SOAs. However, the number of calculations in the SOA IC scheme described here is independent of channel memory and the modulation format and increases linearly with the number of SOAs. For IC of a single SOA in our experiment, the calculations for each symbol of the received signal include merely 64 multiplications, 78 summations, and 20 look-ups.

References

[1] P. I. Kuindersma, G. P. J. M. Cuijpers, J. G. L. Jennen, J. J. E. Ried, L. F. Tiemeijer, H. de Waardt, and A. J. Boot, "10 Gbit/s RZ transmission at 1309 nm over 420 km using a chain of multiple quantum well semiconductor optical amplifier modules at 38 km intervals," in *Proc. ECOC*, 1996, pp. 165–168, Paper TuD.2.1.
[2] G. Onishchukov, V. Lokhnygin, A. Shipulin, and M. Gölles, "Differential binary phase-shift keying transmission using cascaded semiconductor optical amplifiers," in *Proc. CLEO/Pacific Rim*, 1999, pp. 513–514, Paper P.1.97.
[3] L. H. Spiekman, J. M. Wiesenfeld, A. H. Gnauck, L. D. Garrett, G. N. van den Hoven, T. van Dongen, M. J. H. Sander-Jochem, and J. J. M. Binsma, "8 × 10 Gb/s DWDM transmission over 240 km of standard fiber using a cascade of semiconductor optical amplifiers," *IEEE Photon. Technol. Lett.*, vol. 12, no. 8, pp. 1082–1084, Aug. 2000.
[4] Z. Li, Y. Dong, J. Mo, Y. Wang, and C. Lu, "1050-km WDM transmission of 8 × 10.709 Gb/s DPSK signal using cascaded in-line semiconductor optical amplifiers," *IEEE Photon. Technol. Lett.*, vol. 16, no. 7, pp. 1760–1762, Jul. 2004.
[5] X. Li, X. Chen, G. Goldfarb, E. Mateo, I. Kim, F. Yaman, and G. Li, "Electronic post-compensation of WDM transmission impairments using coherent detection and digital signal processing," *Opt. Express*, vol. 16, pp. 880–888, 2008.
[6] G. Goldfarb, M. Taylor, and G. Li, "Experimental demonstration of fiber impairment compensation using the split-step finite-impulse-response filtering method," *IEEE Photon. Technol. Lett.*, vol. 20, no. 22, pp. 1887–1889, Nov. 15, 2008.
[7] G. P. Agrawal and N. A. Olsson, "Self-phase modulation and spectral broadening of optical pulses in semiconductor laser amplifiers," *IEEE J. Quantum Electron.*, vol. 25, no. 11, pp. 2297–2306, Nov. 1989.
[8] J. D. Downie and J. Hurley, "Performance of an MLSE-EDC receiver with SOA-induced nonlinear impairments," *IEEE Photon. Technol. Lett.*, vol. 20, no. 15, pp. 1326–1328, Aug. 1, 2008.